Heterogeneous Catalysis

DOI: 10.1002/ange.200904944

# Super-Resolution Reactivity Mapping of Nanostructured Catalyst Particles**

*Maarten B. J. Roeffaers, Gert De Cremer, Julien Libeert, Rob Ameloot, Peter Dedecker, Anton-Jan Bons, Matthias Bückins, Johan A. Martens, Bert F. Sels, Dirk E. De Vos, and Johan Hofkens**

For almost a century, heterogeneous catalysts have been at the heart of countless industrial chemical processes, but their operation at the molecular level is generally much less understood than that of homogeneous catalysts or enzymes. The principal reason is that despite the macroscopic dimensions of solid catalyst particles, their activity seems to be governed by compositional heterogeneities and structural features at the nanoscale.[1,2] Progress in understanding heterogeneous catalysis thus requires that the nanoscale compositional and structural data[3–5] be linked with local catalytic activity data, recorded in the same small spatial domains and under in situ reaction conditions. Light microscopy is a recent addition to the toolbox for in situ study of solid catalytic materials.[5–7] It combines high temporal resolution and sensitivity with considerable specificity in distinguishing reaction products from reagents. However, lens-based microscopes are subjected to light diffraction which limits the optical resolution to 250 nm in the image plane.[8,9] This resolution is far too limited to resolve the nanosized domains on solid catalysts.

Nanometer-accurate localization of single emitters can be achieved by fitting a Gaussian distribution function to the intensity of the observed fluorescence spot (point-spread function, PSF). This method has been used to map out diffusion pathways in mesoporous or clay materials under highly dilute conditions.[10–12] However, for more concentrated systems, several molecules simultaneously located within a diffraction-limited area cannot be distinguished. Separating the emission of the different fluorescent labels in time, for example by selective photoactivation, solves the problem for imaging of static systems,[8,9,13–18] but not when looking at the dynamics of a working catalyst. Herein, we used single catalytic conversions of small fluorogenic reactants, which occurred stochastically on the densely packed active sites of the catalyst, to reconstruct diffraction-unlimited reactivity maps of catalyst particles. As successive catalytic reactions do not overlap in time, one can precisely determine the location of reaction sites that show turnovers at different moments in time, even if the distance between them is only 10 nm (or less, depending on the signal-to-noise ratio), and reconstruct images of catalytically active zones with super-resolution.

Although fluorogenic substrates are widely used in single-molecule enzymology,[19–23] so far only a few studies have reported single-turnover counting using fluorescence microscopy on solid chemocatalysts.[12,24,25] Such studies typically use large polycyclic substrates, which cannot enter the micropores of many heterogeneous catalysts. Hence, similar experiments on microporous materials critically depend on identifying a small reagent that is converted to a product detectable at the single-molecule level. Surprisingly, furfuryl alcohol is such a reagent, and it appears that after acid-catalyzed reaction (see the Supporting Information),[26,27] the pore-entrapped products are sufficiently fluorescent to be individually observed using a standard microscope equipped with a single excitation source (532 nm diode laser) and sensitive CCD camera (for experimental details, see the Supporting Information). We refer to this novel high-resolution reconstruction method based on catalytic conversion of fluorogenic substrates as NASCA microscopy, or nanometer accuracy by stochastic catalytic reactions microscopy.

Figure 1 a and b show the concept of NASCA microscopy and a 2D fluorescence intensity image of individual product molecules formed by an acid zeolite crystal, respectively. The fluorescence intensity plot of Figure 1 c proves how well the intensity of the individual product molecules allows them to be distinguished from background signals, caused by scatter-

[*] Dr. M. B. J. Roeffaers, Dr. P. Dedecker, Prof. Dr. J. Hofkens
Department of Chemistry, Katholieke Universiteit Leuven
Celestijnenlaan 200F, 3001 Heverlee (Belgium)
Fax: (+32) 163-2799
E-mail: johan.hofkens@chem.kuleuven.be

G. De Cremer, J. Libeert, R. Ameloot, Prof. Dr. J. A. Martens, Prof. Dr. B. F. Sels, Prof. Dr. D. E. De Vos
Department of Microbial and Molecular Systems
Katholieke Universiteit Leuven, Heverlee (Belgium)

Dr. A.-J. Bons
European Technology Center, ExxonMobil Chemical Europe Inc.
Hermeslaan 2, 1831 Machelen (Belgium)

Dr. M. Bückins[+]
Gemeinschaftlabor für Elektronenmikroskopie, RWTH Aachen (Germany)

[+] Current address: Werkstoffkompetenzzentrum, ThyssenKrupp Steel AG
Kaiser-Wilhelm-Strasse 100, 47166 Duisburg (Germany)

[**] M.B.J.R., G.D.C., R.A., and P.D. thank the FWO (Fonds voor Wetenschappelijk Onderzoek)-Flanders for PhD or postdoctoral fellowships. This work was performed within the framework of the IAP-VI program Functional Supramolecular Systems of the Belgian Federal Government. The authors acknowledge financial support from the FWO Flanders (Grants G.0366.06 and G.0402.09), the K. U. Leuven Research Fund (GOA 2006/2, Center of Excellence CECAT, CREA2007), the Flemish Ministry of Education (ZWAP 04/007), long-term structural funding "Methusalem" by the K. U. Leuven, and the European Network of Excellence (IDECAT). This work was supported by the EC 6th Framework Program (ERAS-CT-2003-980409).

Supporting information for this article is available on the WWW under http://dx.doi.org/10.1002/anie.200904944.

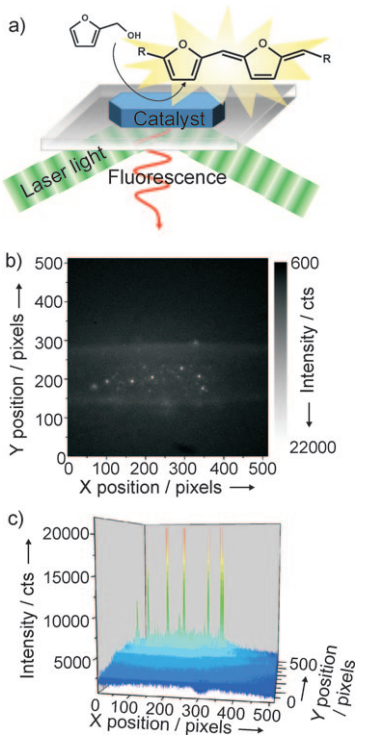


***Figure 1.*** a) Concept of NASCA microscopy. b) Wide-field fluorescence micrograph showing spatially resolved individual catalytic conversions of furfuryl alcohol on a micrometer-sized ZSM-5 zeolite crystal. c) Intensity profile of the crystal from (b), which demonstrates the highly intense signals that can be obtained.

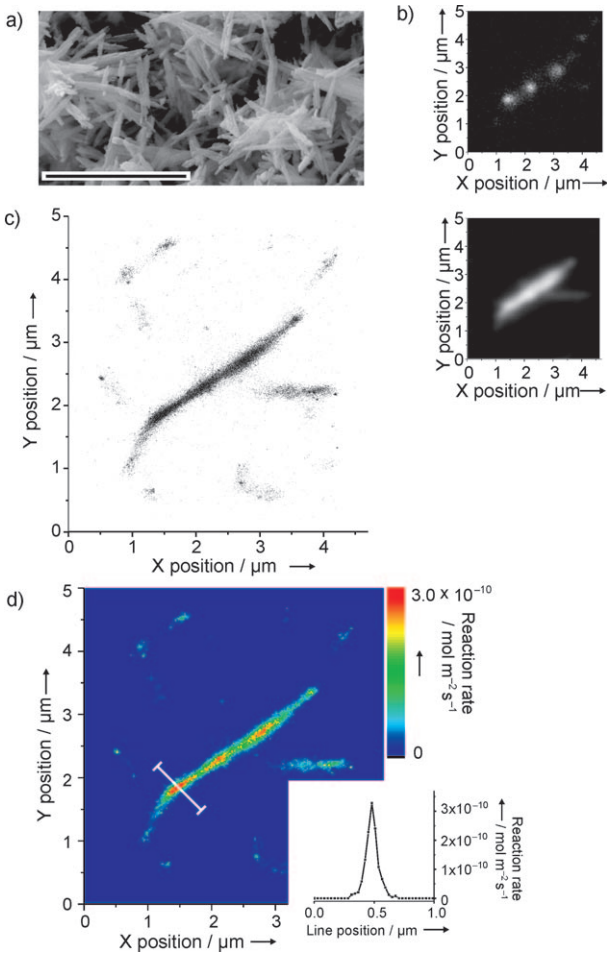


***Figure 2.*** a) SEM image of needle-like ZSM-22 crystallites. The average width of the particles is 120 nm. Scale bar: 5 µm. b) Individual and spatially resolved catalytic conversions of furfuryl alcohol on an isolated ZSM-22 crystallite (top) and the diffraction-limited image (bottom) resulting from accumulation of all fluorescence observed during a 1000 s reaction on the crystallite (10000 frames). c) Scatter plot of all identified reaction spots on the same particle as in (b). d) Reaction map calculated for $20\times20$ nm$^2$ pixels using the data in (c). The inset shows the local reaction rate as measured along the white line (see also the Supporting Information, Figure S2).

ing or by emission from reagent molecules, even at furfuryl alcohol concentrations as high as 1M.

As a first case study, we investigated the catalytic activity of ZSM-22 zeolite particles. This ten-membered-ring (10-MR) zeolite with unidimensional channels typically occurs as needle-like crystallites with widths well below the classic diffraction limit (Figure 2a). Figure 2b shows three well-separated single catalytic turnovers on an isolated ZSM-22 needle in a single frame. For a movie recorded for 1000 s, the accumulated fluorescence intensity image shows the ZSM-22 particle as an object broadened to approximately 500 nm as a direct result of diffraction (see the Supporting Information). In contrast, by precise mathematical localization of all individual catalytic reaction centers[28] and subsequent reconstruction (see the Supporting Information), an optical image is obtained showing the isolated needle with its real width of about 100 nm (Figure 2c).

Furthermore, nanometer-scale kinetics can be mapped by counting the number of catalytic conversions in a selected area of arbitrary size. Figure 2d shows such a kinetic map with reaction turnovers binned in $20\times20$ nm$^2$ pixels. This reveals zones with different activity within one ZSM-22 rod. In this specific case the activity is spaced along the long axis of the rod in three zones (Figure 2d). This observation is in line with the notion of the aggregative growth of ZSM-22.[29] In this process, silica is first oligomerized around molecular templates and forms discrete aluminum-containing nanorods. Oriented aggregation of these nanorods results in crystallites that contain catalytic activity even in the center of the aggregate, as is clearly seen in Figure 2d. This kinetic map demonstrates that NASCA microscopy is an organic counterpart of the recently reported nanoscale mapping of inorganic catalyst compositions,[3] and adds unique information on the local catalytic activity.

In a second case study, micrometer-sized crystals of ZSM-5 were examined. Perfect ZSM-5 crystals should contain straight and sinusoidal 10-MR pores that are perpendicular to one another. However, detailed structural characterization by focused-ion-beam (FIB) milling and electron microscopy (for experimental details, see the Supporting Information) shows that at the nanoscale, the crystals are more complex (Figure 3). Starting from a seemingly perfect crystal (Figure 3a), two thin sections were generated by FIB milling (Figure 3b) and transferred to a transmission electron microscope (Figure 3c).

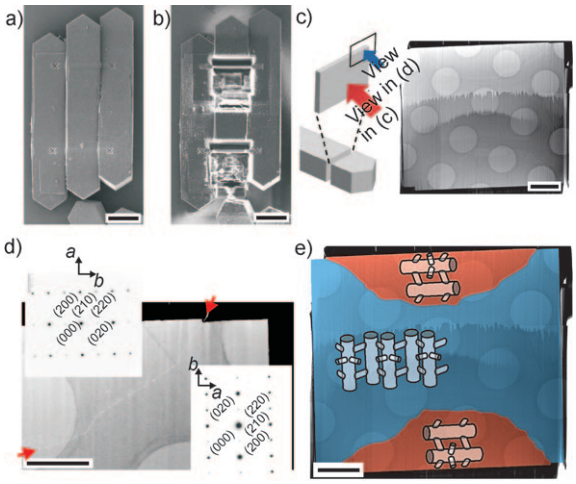


***Figure 3.*** a) Secondary electron image of three adjacent crystals in the FIB after Au/W coating, and after applying the reference marks for the FIB process. Scale bar: 5 μm. b) FIB sections through the middle crystal, prior to lift-out. Scale bar: 5 μm. c) Schematic representation of the FIB–transmission electron microscopy (TEM) approach (left), and high-angle annular dark-field scanning TEM image of the same section (right; scale bar: 2 μm). The black rim is the metal coating, and the circular features are the holes in the Quantifoil support film. Other contrast features in the section are thickness variations arising from FIB artifacts (vertical striations and stepwise increase in thickness from the top to the bottom of the image). d) Detail of the top-right corner of the section, which shows the interface running as a white line from a small ledge in the surface into the crystal to the bottom left (marked with red arrows). Scale bar: 1 μm. Insets: electron diffraction patterns from the two zones, which show that the crystallographic *a* axis is vertical in the top left and horizontal in the bottom right. e) Summary of the FIB-TEM observations, with the crystal orientation indicated by color and by a schematic representation of the channel system. Scale bar: 2 μm.

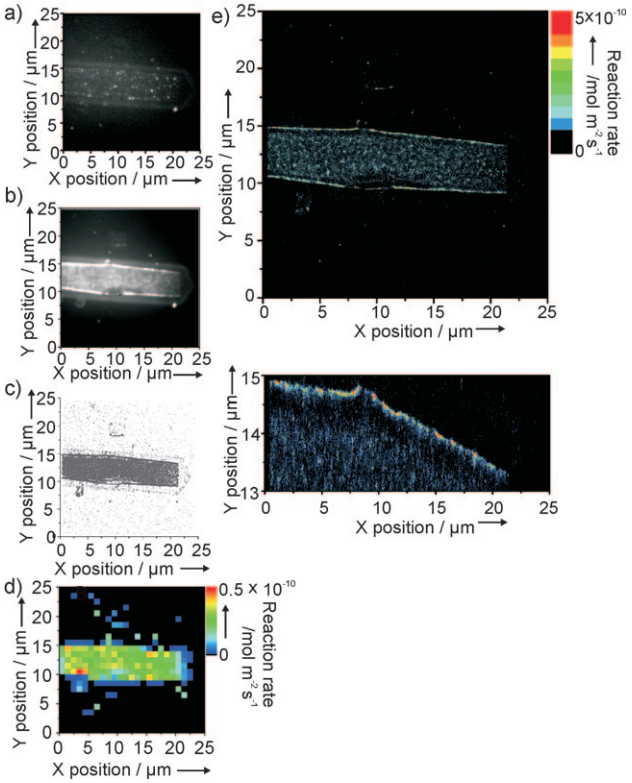


***Figure 4.*** a) Individual fluorescent product molecules on a ZSM-5 crystal. The contours of the crystal are visible because of a small amount of unfiltered scattered light. b) Accumulated and diffraction-limited image of all reactions observed during the time course of the recorded movie (80 s, 800 frames). c) Reconstructed image obtained after mathematical fitting of all reaction events observed in the 800-frame movie. d) Resolved reaction map ($1\times1$ μm$^2$) reconstructed using the data in (c). e) Similar resolved reaction map (top) calculated for $20\times20$ nm$^2$ pixels with a zoom (bottom) at the upper part of the active rim.

The top and bottom parts of these sections originate from the hexagonal facet of the ZSM-5 crystal. Zooming in on the top-right corner of the section (Figure 3d) reveals a clear 60 nm step on the hexagonal facet. In the sectional view of the crystal (Figure 3d and e), a clear line starts at this surface step, runs through the interior of the crystal, and reappears at the left-hand side of the same crystal facet, where a similar surface step is observed. Electron diffraction patterns taken from two representative crystal zones prove that the line-like feature is actually an interface between two zones with different crystallographic orientation (Figure 3d and e). This type of 90° intergrowth has often been proposed for ZSM-5 crystals,[27,30–34] but the activity of the resulting nanosteps in a catalytic reaction has never been measured.

For nanoscale reactivity mapping of ZSM-5, the same furfuryl alcohol oligomerization as for Figures 1 and 2 was used to look in detail at the hexagonal facet of a ZSM-5 crystal. The single frame of Figure 4a shows individual well-resolved catalytic turnovers with high signal-to-noise ratio. A movie was recorded in the first 80 s of the reaction, just after adding furfuryl alcohol to the crystals submerged in water (Supporting Information, Movie SI-1). By accumulating data from the movie, a diffraction-limited fluorescence intensity image (Figure 4b) and a map of the fitted reaction centers (Figure 4c) were generated. The heterogeneity in catalytic activity can be quantified by binning the precisely localized individual reaction turnovers from Figure 4c into well-defined pixels of area $1\times1$ μm$^2$ or $20\times20$ nm$^2$. Reaction data plotted on the micrometer scale show that there are few product molecules at the periphery of the hexagonal facet (Figure 4d), and deceptively suggest that the activity is evenly distributed over a quasi-rectangular part in the middle of the facet, which corresponds to the micrometer-sized 90° intergrown section. However, the surface nanosteps are not resolved. The true power of our nanoscale reactivity mapping is revealed when data are binned into $20\times20$ nm$^2$ pixels. This super-resolution kinetic map (Figure 4e and zoom) uncovers a very narrow (20–60 nm wide) exceedingly active zone at the boundary of the 90° intergrowth, where reaction rates are at least ten times more elevated. The resolution that can currently be achieved with NASCA microscopy is 10 nm (see the Supporting Information).

A zoom-in at the active rim in Figure 4e also unveils nanometer-sized structural kinks in the seemingly straight edge. When relating these fluorescence-microscopy-based reactivity data to the structural information of Figure 3, the

significance of the highly active rim becomes clear: at the edges of the 90° intergrown crystal part, that is, at the 50–100 nm surface steps, locally there is reagent influx from two crystal faces via both the sinusoidal and the straight pores. This explains the very high catalytic activity observed at the edge of the intergrowth. With traditional light microscopy techniques, such a narrow zone of elevated activity remains unnoticed because of the diffraction-limited resolution. Secondly, the observed kinks on the surface step are in agreement with the current view on ZSM-5 growth through incorporation of pentasil chains. AFM has proven that this growth process is prone to defect incorporation, and this results in irregularities in the developing crystal edge.[30,35,36]

In summary, the new NASCA microscopy approach records organic reactivity maps of catalysts at small length scales similar to those of electron, scanning probe, or X-ray microscopy, which rather give inorganic or structural information. This labeling-free scheme is based on conversion of single fluorogenic molecules on the true active sites, and has a generic character as it is broadly applicable, even in biological samples. The approach is technically easy since only one excitation wavelength is necessary and since a spatiotemporal overlap between different lasers, as required in most other fluorescence nanomicroscopy approaches, is not required.[8,9,13–15] Simple adjustment of the concentration of the fluorogenic substrate to the catalytic activity and adaptation of the laser power employed, to ensure high signal-to-noise ratio readout and subsequent photobleaching, are sufficient to limit the number of detected events to one per diffraction-limited area. One general concern in all types of reconstruction optical microscopy is whether the labeling density is sufficient for proper imaging of the structure under investigation, following the so-called Nyquist criterion.[13] In the current experiments this is not an issue since active sites are abundantly present (see the Supporting Information). Three-dimensional visualizations can be readily achieved (Supporting Information, Movie SI-2). An improved *Z* resolution can be expected when applying, for example, biplane imaging[37] or two-photon excitation,[38] since bleaching is not a limiting factor in this assay. This last option also opens the possibility to investigate processes deeply buried within catalyst beds.

Received: September 3, 2009
Published online: November 4, 2009

**Keywords:** fluorescence · heterogeneous catalysis · kinetics · single-molecule studies · zeolites

[1] D. R. Rolison, *Science* **2003**, *299*, 1698.
[2] H. Kato, K. Asakura, A. Kudo, *J. Am. Chem. Soc.* **2003**, *125*, 3082.
[3] E. de Smit, I. Swart, J. F. Creemer, G. H. Hoveling, M. K. Gilles, T. Tyliszczak, P. J. Kooyman, H. W. Zandbergen, C. Morin, B. M. Weckhuysen, F. M. F. de Groot, *Nature* **2008**, *456*, 222.
[4] J. W. Niemantsverdriet, *Spectroscopy in Catalysis: An Introduction*, 3rd ed., Wiley-VCH, Weinheim, **2007**.
[5] B. M. Weckhuysen, *Angew. Chem.* **2009**, *121*, 5008; *Angew. Chem. Int. Ed.* **2009**, *48*, 4910.
[6] M. B. J. Roeffaers, G. De Cremer, H. Uji-i, B. Muls, B. F. Sels, P. A. Jacobs, F. C. De Schryver, D. E. De Vos, J. Hofkens, *Proc. Natl. Acad. Sci. USA* **2007**, *104*, 12603.
[7] M. B. J. Roeffaers, J. Hofkens, G. De Cremer, F. C. De Schryver, P. A. Jacobs, D. E. De Vos, B. F. Sels, *Catal. Today* **2007**, *126*, 44.
[8] S. W. Hell, *Science* **2007**, *316*, 1153.
[9] S. W. Hell, *Nat. Methods* **2009**, *6*, 24.
[10] A. Zürner, J. Kirstein, M. Doblinger, C. Braeuchle, T. Bein, *Nature* **2007**, *450*, 705.
[11] J. Kirstein, B. Platschek, C. Jung, R. Brown, T. Bein, C. Brauchle, *Nat. Mater.* **2007**, *6*, 303.
[12] M. B. J. Roeffaers, B. F. Sels, H. Uji-i, F. C. De Schryver, P. A. Jacobs, D. E. De Vos, J. Hofkens, *Nature* **2006**, *439*, 572.
[13] E. Betzig, G. H. Patterson, R. Sougrat, O. W. Lindwasser, S. Olenych, J. S. Bonifacino, M. W. Davidson, J. Lippincott-Schwartz, H. F. Hess, *Science* **2006**, *313*, 1642.
[14] M. J. Rust, M. Bates, X. W. Zhuang, *Nat. Methods* **2006**, *3*, 793.
[15] M. Heilemann, P. Dedecker, J. Hofkens, M. Sauer, *Laser Photonics Rev.* **2009**, *3*, 180.
[16] M. Heilemann, S. van de Linde, M. Schuttpelz, R. Kasper, B. Seefeldt, A. Mukherjee, P. Tinnefeld, M. Sauer, *Angew. Chem.* **2008**, *120*, 6266; *Angew. Chem. Int. Ed.* **2008**, *47*, 6172.
[17] M. Heilemann, S. van de Linde, A. Mukherjee, M. Sauer, *Angew. Chem.* **2009**, *121*, 7036; *Angew. Chem. Int. Ed.* **2009**, *48*, 6903.
[18] J. Vogelsang, T. Cordes, C. Forthmann, C. Steinhauer, P. Tinnefeld, *Proc. Natl. Acad. Sci. USA* **2009**, *106*, 8107.
[19] K. Blank, G. De Cremer, J. Hofkens, *Biotechnol. J.* **2009**, *4*, 465.
[20] G. De Cremer, M. B. J. Roeffaers, M. Baruah, M. Sliwa, B. E. Sels, J. Hofkens, D. E. De Vos, *J. Am. Chem. Soc.* **2007**, *129*, 15458.
[21] B. P. English, W. Min, A. M. van Oijen, K. T. Lee, G. B. Luo, H. Y. Sun, B. J. Cherayil, S. C. Kou, X. S. Xie, *Nat. Chem. Biol.* **2006**, *2*, 87.
[22] S. Kuznetsova, G. Zauner, T. J. Aartsma, H. Engelkamp, N. Hatzakis, A. E. Rowan, R. J. M. Nolte, P. C. M. Christianen, G. W. Canters, *Proc. Natl. Acad. Sci. USA* **2008**, *105*, 3250.
[23] S. Rocha, J. A. Hutchison, K. Peneva, A. Herrmann, K. Muellen, M. Skjot, C. I. Jorgensen, A. Svendsen, F. C. De Schryver, J. Hofkens, H. Uji-i, *ChemPhysChem* **2009**, *10*, 151.
[24] V. M. Martinez, G. De Cremer, M. B. J. Roeffaers, M. Sliwa, M. Baruah, D. E. De Vos, J. Hofkens, B. F. Sels, *J. Am. Chem. Soc.* **2008**, *130*, 13192.
[25] W. Xu, J. S. Kong, Y.-T. E. Yeh, P. Chen, *Nat. Mater.* **2008**, *7*, 992.
[26] M. Choura, N. M. Belgacem, A. Gandini, *Macromolecules* **1996**, *29*, 3839.
[27] M. B. J. Roeffaers, B. F. Sels, H. Uji-i, B. Blanpain, P. L'Hoest, P. A. Jacobs, F. C. De Schryver, J. Hofkens, D. E. De Vos, *Angew. Chem.* **2007**, *119*, 1736; *Angew. Chem. Int. Ed.* **2007**, *46*, 1706.
[28] M. K. Cheezum, W. F. Walker, W. H. Guilford, *Biophys. J.* **2001**, *81*, 2378.
[29] K. Hayasaka, D. Liang, W. Huybrechts, B. R. De Waele, K. J. Houthoofd, P. Eloy, E. M. Gaigneaux, G. van Tendeloo, J. W. Thybaut, G. B. Marin, J. F. M. Denayer, G. V. Baron, P. A. Jacobs, C. E. A. Kirschhock, J. A. Martens, *Chem. Eur. J.* **2007**, *13*, 10070.
[30] M. B. J. Roeffaers, R. Ameloot, M. Baruah, H. Uji-i, M. Bulut, G. De Cremer, U. Müller, P. A. Jacobs, J. Hofkens, B. E. Sels, D. E. De Vos, *J. Am. Chem. Soc.* **2008**, *130*, 5763.
[31] M. B. J. Roeffaers, R. Ameloot, A.-J. Bons, W. Mortier, G. De Cremer, R. de Kloe, J. Hofkens, D. E. De Vos, B. F. Sels, *J. Am. Chem. Soc.* **2008**, *130*, 13516.
[32] M. H. F. Kox, E. Stavitski, B. M. Weckhuysen, *Angew. Chem.* **2007**, *119*, 3726; *Angew. Chem. Int. Ed.* **2007**, *46*, 3652.
[33] L. Karwacki, E. Stavitski, M. H. F. Kox, J. Kornatowski, B. M. Weckhuysen, *Angew. Chem.* **2007**, *119*, 7366; *Angew. Chem. Int. Ed.* **2007**, *46*, 7228.

  

[34] E. Stavitski, M. H. F. Kox, B. M. Weckhuysen, *Chem. Eur. J.* **2007**, *13*, 7057.
[35] J. R. Agger, N. Hanif, C. S. Cundy, A. P. Wade, S. Dennison, P. A. Rawlinson, M. W. Anderson, *J. Am. Chem. Soc.* **2003**, *125*, 830.
[36] L. I. Meza, M. W. Anderson, J. R. Agger, C. S. Cundy, C. B. Chong, R. J. Plaisted, *J. Am. Chem. Soc.* **2007**, *129*, 15192.
[37] M. F. Juette, T. J. Gould, M. D. Lessard, M. J. Mlodzianoski, B. S. Nagpure, B. T. Bennett, S. T. Hess, J. Bewersdorf, *Nat. Methods* **2008**, *5*, 527.
[38] J. Fölling, V. Belov, R. Kunetsky, R. Medda, A. Schonle, A. Egner, C. Eggeling, M. Bossi, S. W. Hell, *Angew. Chem.* **2007**, *119*, 6382; *Angew. Chem. Int. Ed.* **2007**, *46*, 6266.

  